



CrossMark
 click for updates

Cite this: *RSC Adv.*, 2016, 6, 27669

Flame-retardant, electrically conductive and antimicrobial multifunctional coating on cotton fabric *via* layer-by-layer assembly technique

Xiaoxuan Chen,^{ab} Fei Fang,^c Xian Zhang,^{*a} Xin Ding,^a Yanyan Wang,^a Lin Chen^a and Xingyou Tian^{*a}

A multifunctional coating composed of polyhexamethylene guanidine phosphate (PHMGP) and potassium alginate-carbon nanotubes (PA-CNTs) was constructed on cotton fabric *via* a layer-by-layer assembly technique. The growth of the assembly coating was monitored by Fourier transform infrared spectroscopy and the result shows the assembly coating grows approximately linearly with the increase of bilayer number. The electrical conductivity test shows that the assembly coating endows cotton with electrical conductivity, due to the formation of a CNT network on the cotton fabric. The thermo-stability and flame resistance were evaluated by thermo-gravimetric analysis and a vertical flammability test, and the results indicate that the assembly coating promotes char formation, decreases the burning time and eliminates the afterglow during combustion. The antimicrobial assessment suggests that the assembly coating can effectively inhibit the growth of *Escherichia coli*, and the inhibiting effect increases with the growth of bilayer number. A multifunctional cotton fabric could be produced by the LBL assembly technique, which enlarges its application area.

Received 16th December 2015
 Accepted 14th February 2016

DOI: 10.1039/c5ra26914h

www.rsc.org/advances

Introduction

For the past few years, the layer-by-layer (LBL) assembly technique has been regarded as one of the most popular methods to fabricate functional composite coatings. It was first suggested by R. Iler in 1966,¹ and involves the alternative deposition of oppositely charged colloids. In the early 1990s, Decher and coworkers rediscovered LBL assembly to prepare a polyelectrolyte multilayer thin film and began to recognize the significance of this technique.²⁻⁴ LBL assembly involves the alternate absorption of species to form composite multilayer coating by electrostatic attractions, hydrogen-bonds, and coordination bonds, *etc.*⁵⁻⁸ The building species of LBL multilayer include polyelectrolyte, nano-particles and complexes of these materials.^{9,10} To fabricate multilayer coatings, a charged substrate was alternately immersed into cationic and anionic aqueous solutions, then rinsed with water and dried in air. Hence, LBL assembly can be identified as a simple, inexpensive and versatile technique, which has been widely applied in preparation of various functional coatings.¹¹

Cotton textiles are widely used in daily life, and have different functional requirements in different application area. Considering the need of safety, flame retardant property of cotton fabric must be realized. In 2011, Grunlan *et al.* had constructed intumescent flame retardant coating composed of poly(sodium phosphate) and poly(allylamine) on cotton fabric to achieve self extinguishing during vertical flammability test.¹² Since then, lots of efforts have been devoted to further perfect the fire performance. For instance, Galina Laufer and coworkers used positively charged chitosan and anionic montmorillonite as the coating materials, and further investigated the influence of changing PH on the coating thickness and flame retardant property.¹³ Nowadays, numbers of workers aim at green composition and degradable coating materials; to this purpose, DNA and chitosan have been used to endow cotton with flame retardant properties.¹⁴ Alginate extracted from brown algae, as a kind of green composition, has a vast development potential which was reported to have high limited oxygen index (LOI).¹⁵ Meanwhile, antimicrobial cotton fabrics are gradually concerned in the need of health. Dubas *et al.* had prepared antimicrobial nylon and silk fibers by introducing silver nanoparticles to the multilayer assembly coating.¹⁶ Additionally, in order to enlarge its application area, some other functional cotton fabrics yet have been greatly developed, such as UV resistance, superhydrophobic property, and so on. According to the above report, various function multilayer coating could be formed on textile fiber surface by LBL assembly process.¹⁷⁻¹⁹ However, it is noteworthy that there are few reports about

^aInstitute of Applied Technology, Hefei Institutes of Physical Science, Chinese Academy of Sciences, Hefei 230088, People's Republic of China. E-mail: xzhang@issp.ac.cn; xytian@issp.ac.cn; Fax: +86-551-65393564; Tel: +86-551-65592752

^bUniversity of Science and Technology of China, Hefei 230026, People's Republic of China

^cInstitute of Plasma Physics, Chinese Academy of Sciences, Hefei 230031, People's Republic of China

simultaneously endowing textile fabric multifunction, such as electrical, antimicrobial and flame retardant property.

It may be a feasible solution by respectively selecting different functional cationic and anionic polyelectrolyte layers during the LBL assembly process. Poly(hydroxamic acid) and poly(*N*-vinylguanidine) were constructed on polyacrylonitrile fiber surface by LBL assembly technique and successfully endowed the fiber sample with good air permeability and antibacterial property.²⁰ The fabric coated with the chitosan, poly(sodium phosphate) and a conductive recipe composed of poly(diallyldimethylammonium chloride) and multiwalled carbon nanotubes exhibited noticeable flame retardant and conductivity.²¹ In our previous report,²² polyhexamethylene guanidine phosphate–ammonium polyphosphate (PHMGP–APP) assembly coating was constructed to simultaneously endow cotton fabric with flame retardant and antimicrobial property. On one hand, PHMGP can endow cotton with antimicrobial property by electrostatic linking with the anionic carboxylate groups on cotton. On the other hand, PHMGP–APP assembly coating constitutes an efficient intumescent flame retardant system and has played an excellent fire resistant performance in consideration of the health need, very recently, environmentally friendly PHMGP–potassium alginate assembly coating (PHMGP–PA) was further constructed for flame retardant and antimicrobial cotton fabric.²³ However, the property of PHMGP–PA coating is not as good as that of PHMGP–APP coating, especially the fire resistant performance.

As an intrinsic conductive material, CNTs have also been verified as a new inorganic flame retardant and play a role of physical barrier during the combustion process.²⁴ Therefore, an electrical coating can be theoretically realized by incorporation of CNTs to PHMGP–PA assembly multilayer coating. In comparison of our previous work,²³ on one hand, the antimicrobial and flame retardant cotton fabric could be further endowed with electrical conductive property, which may enlarge the application scope of cotton fabric. For example, LBL assembled electrical conductive fabrics could be used as sensors.²⁵ On the other hand, the fire resistant performance could be further improved by combination of mechanism of intumescent flame retardant and physical barrier. More importantly, PA could be employed to improve the poor dispersibility of CNTs in water in the manner of hydrogen bond²⁶ and formed PA–CNTs anion hybrid electrolyte.

In present study, PHMGP/PA–CNTs assembly coating was constructed on cotton fabric to simultaneously achieve electrical, antimicrobial and flame retardant property. Fourier transform infrared spectroscopy was conducted to confirm the presence and growth of the assembly coating on cotton. The electrical conductivity, flame retardant and antimicrobial properties were measured by four probe methods, vertical flammability test and Kirby–Bauer test, respectively.

Experiments

Materials

Alginate potassium (300–800 mPa s) was supplied by Qingdao Bright Moon seaweed Group Co., Ltd. PHMGP solution (25%,

$n > 60$) was purchased from Shanghai Scunder Industry Co., Ltd. Cotton fabric (230 g m^{-2}) was supplied by a textile fabrics store. CNTs (OD: 10–20 nm, L : 10–30 μm) were offered by XFNANO Advanced Materials Supplier.

LBL assembly process

0.1 wt% cationic PHMGP and 0.1 wt% anionic PA aqueous solution were respectively prepared. Then, 0.5 g CNTs were added into 500 mL PA aqueous solution and ultrasonic dispersed for 4 h. Finally, stable PA–CNTs suspension was formed by removing sediment of a part of CNTs after 2 days.

Cotton fabric was immersed in deionized water and dried in air as pretreatment. Then it was alternatively immersed into cationic PHMGP and anionic PA–CNTs suspension. After each immersion, cotton fabric was rinsed by deionized water for 2 min and then dried in air at 70 °C for 30 min. The initial two immersion times are 5 min to promote the electrostatic adsorption of PHMGP and PA on cotton fiber and the subsequent immersion time is 1 min. Once the desired bilayer (BL) number (5BL, 10BL and 20BL) was respectively achieved, the coated fabric was dried in air at 70 °C for 50 min.

Measurement and characterization

Fourier transform infrared spectra were conducted on a Nicolet 8700 spectrometer (Thermo Nicolet Corporation, USA, 32 scans and 4 cm^{-1} resolution).

Surface morphologies of the control and coated cotton fabrics were imaged by a Sirion 200 field emission scanning electron microscope (SEM) (FEI Corporation, USA). Before observation, all samples were gold sprayed.

Electrical conductivities of all samples were measured by RTS-9 double electric logging four point probe tester (Uncommon (Tianjin) Sci. & Tech. Development Co., Ltd).

Thermo gravimetric analyses of all fabrics were recorded by a Pyris 1 TGA from 50 °C to 600 °C at a heating rate of $10 \text{ }^\circ\text{C min}^{-1}$ under air atmosphere (PerkinElmer, USA, air flux: 40 mL min^{-1}). The experimental error was $\pm 1 \text{ }^\circ\text{C}$ for temperature and $\pm 0.1\%$ for residual mass.

The combustion behaviors of all fabrics were observed on an AG5100A Horizontal vertical flame tester (Zhuhai Angui Testing Instrument Co., Ltd), according to GB/T 5455-1997.

The antimicrobial ability of coated fabrics was measured *via* the Kirby–Bauer test. *E. coli* which is Gram-negative bacterium was selected to be pathogenic bacterium in the test. Nummular piece which radius is 4 mm was cut from each coated fabric. A beef extract as culture medium was placed in Petri dishes, and *E. coli* was sprinkled homogeneously on the surface of beef extract. Putting the nummular pieces and the Petri dishes were put in an incubator at 37 °C for 24 h at last.

In order to quantitatively assess the antimicrobial ability of PHMGP/PA–CNTs coating, we adopted a modified AATCC test method 100-2004 which was designed for the dissolving type antimicrobial fabric. $1 \text{ cm} \times 1 \text{ cm}$ fabrics were infiltrate with $100 \mu\text{L}$ of 2×10^5 *E. coli* and kept for 30 min or 60 min at 37 °C. Then all samples were ultrasonic treated for 1 min and vortexed

for 2 min in 10 mL sterile water. Samples were diluted serially and coated on tryptose agar. Then cultivated at 37 °C for 24 h.

Results and discussion

Surface composition

The chemical compositions of different fabrics were investigated by ATR-FTIR spectroscopy and the corresponding spectra were shown in Fig. 1. Pure cotton fabric presents the characteristic signals of cellulose.²⁷ Two absorption peaks at 3347 and 2908 cm^{-1} are attributed to the -OH stretching and C-H of aliphatic stretching vibration, respectively. Additionally, there appear two fingerprint peaks around 1372–1316 cm^{-1} and 1162–1033 cm^{-1} corresponding to the -OH in-plane and C-O bending vibration,²⁸ respectively. The coated fabrics also present similar characteristic signals of cellulose, overlapping with the control sample. However, there appear two new absorption peaks at 1634 cm^{-1} and 1595 cm^{-1} assigned to the N-H bending vibration of PHMGP²⁹ and -COO symmetrical stretching vibration of PA,³⁰ respectively, suggesting the presence of PHMGP and PA on the fabric surface. Furthermore, the intensity of absorption peaks increases with the increasing of bilayer number.

To further monitor the growth process of coating on fabric, the absorption value at 1056 cm^{-1} of C-O-C is chosen as the reference, the relative absorption values (N-H/C-O-C absorbance ratio: $A_{1634 \text{ cm}^{-1}}/A_{1056 \text{ cm}^{-1}}$, -COO/C-O-C absorbance ratio: $A_{1595 \text{ cm}^{-1}}/A_{1056 \text{ cm}^{-1}}$), are calculated as functions of the bilayer number, the functional image was inserted in Fig. 1. It can be found that the relative absorption values present approximately linearly growth with the increase of bilayer number, which indicates that the quantities of PHMGP and PA both linearly grow in the LBL assembly process.

The morphologies of the different fabrics samples were observed by SEM. As shown in Fig. 2, the uncoated sample has

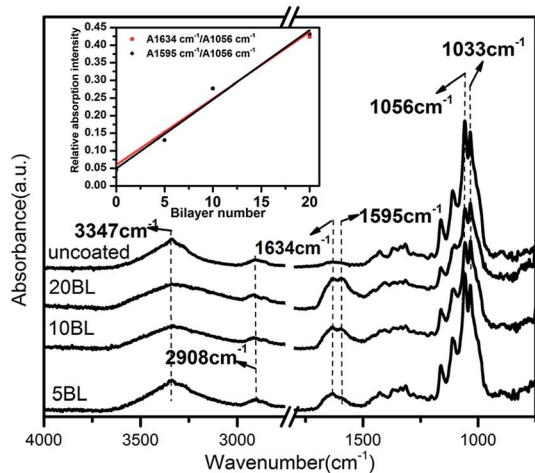


Fig. 1 ATR-FTIR spectra of the control and coated fabrics. The inset image shows the relative absorption values of $A_{1634 \text{ cm}^{-1}}/A_{1056 \text{ cm}^{-1}}$ and $A_{1595 \text{ cm}^{-1}}/A_{1056 \text{ cm}^{-1}}$ as function of bilayer number.

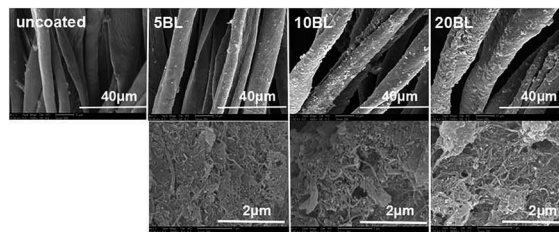


Fig. 2 SEM images of all fabrics samples before VFT.

a smooth surface. By deposited the assembly coating, the coated fabrics show a rough surface. Moreover, the coating thickness increases with the increasing of the bilayer number. At higher magnification, it could be found that CNTs networks appear on the surface of the coated fabric. In consideration of the characteristic of electric conductivity, the assembly coating filled with CNTs network could act as a conductive coating. As shown in Fig. 3, the coated fabrics possess excellent electric conductivity and the conductivity increases with the bilayer number. Pure cotton has an electric conductivity of $10^{-13} \text{ S m}^{-1}$. After coated with 5BL coating, the electric conductivity increases to $10^{-12} \text{ S m}^{-1}$. With the bilayer number increasing to 10, the conductivity increases to 10^{-5} S m^{-1} , enhanced by seven orders of magnitude. As for the fabric sample with 20BL number, the conductivity reaches up to 10^{-2} S m^{-1} . The enhanced electric conductivity could be attributed to the higher cross-linking degree of CNTs in the assembly coating on fabric, also further indicating the quantity of CNTs grow in the LBL assembly coating.

Thermal properties

The thermal stabilities of the pure and coated fabrics were evaluated by TGA under air atmosphere, and the corresponding curves and collected data were shown in Fig. 4 and listed in Table 1. Pure cotton begins to decompose at 337 °C due to the depolymerization of cellulose and exhibits the maximum weight loss rate at 362 °C in the first stages, 200–400 °C. Then, the formed aliphatic char is gradually converted into aromatic

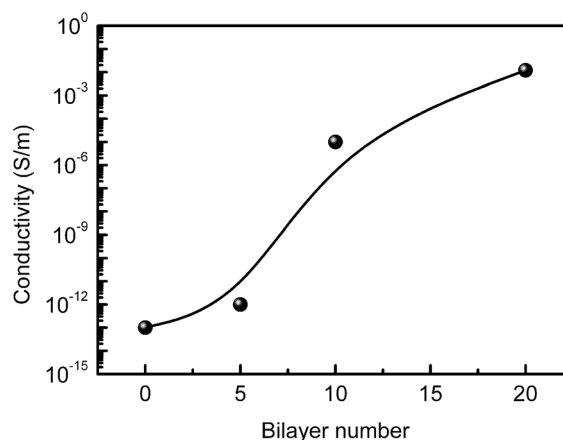


Fig. 3 The electric conductivity as a function of the bilayer number.

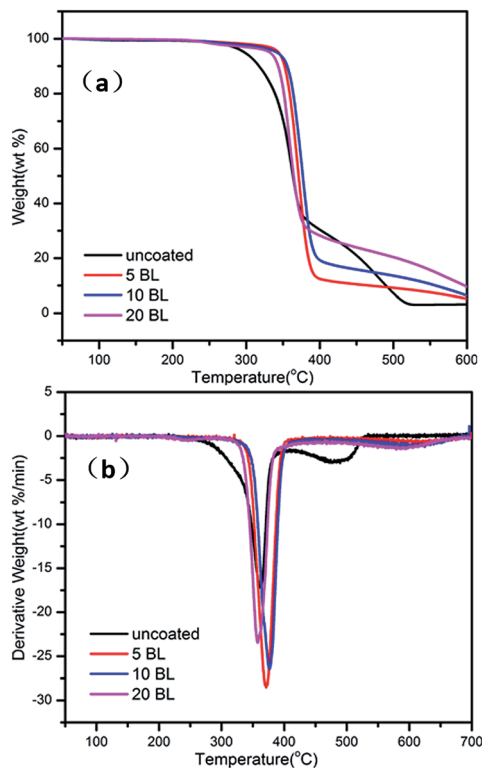


Fig. 4 (a) TG curves and (b) DTG curves of all fabrics samples.

char and simultaneously oxidized to generate volatile gases CO_2 and CO^{31} in the second stage, 400–600 °C. Just like the uncoated sample, the coated fabrics also show two decomposition stages. However, the first decomposition stage is obviously delayed by introducing the PHMGP/PA-CNT assembly coating, which can be confirmed by the increased T_{onset} and $T_{\text{max}1}$, as listed in Table 1. As previous reported results suggested,²² the thermally decomposition products from PA protect cotton from firing in the initial decomposition stage. In present system, the incorporation of CNTs, as inorganic nano-material, also contribute to the increase of thermal stability of cotton fabric.³² Then, thanks to the delay effect, the decomposition of cotton can be catalyzed by the released phosphoric acid from synchronous decomposition of PHMGP. The catalytic action of PHMGP can further facilitate the formation of char, which makes coated fiber be more thermally stable at higher temperatures. As shown in Fig. 4, the coated fabrics present increased $T_{\text{max}2}$ and more residual char at 500 and 600 °C. Significantly, the residue masses increase with the increase of bilayer number, indicating

an enhanced charring effect of the assembly coating with more bilayer numbers. Additionally, the mass of residual char is much higher than the coating increment, suggesting that residue left mainly comes from cotton substrate. Besides the catalytic effect of PHMGP-PA system, CNTs also have an important effect on the decomposition process: one is to further improve the thermal stability of uncoated sample in the first stage, and favors the occurrence of catalytic action due to the higher decomposition temperature of PHMGP than that of uncoated sample. The other one is that CNTs also act as a physical barrier of thermal and oxygen to improve the stability of cotton in the second stage, apart from the formed intumescent char by PHMGP-PA system.²³

Fire resistant performance

The combustion behaviors of all fabrics were recorded by VFT and the pictures of the scene at 10 and 25 s are shown in Fig. 5. The combustion behavior of all samples was reflected in Table 2. Pure cotton burned vigorously with the red light after it was exposed to direct fire source, and the flame lasted for 27 s. After it was extinguished, there appeared 18 s afterglow phenomenon. By depositing with the assembly coating, cotton fabric burned with a dim flame in shorter time. The 5 and 10BL samples presented 23 s burning time. As the bilayer number increasing to 20, the burning time decreased to 22 s. Furthermore, there is no afterglow phenomenon appeared on the coated fabrics during combustion. After VFT testing, the uncoated fabric consumed completely without any residue left. However, the coated fabric left residue with unbroken fabric structure, as shown in Fig. 6. Moreover, the mass of residue char increases with the increase of bilayer number. The above results indicate that the assembly coating performs good flame

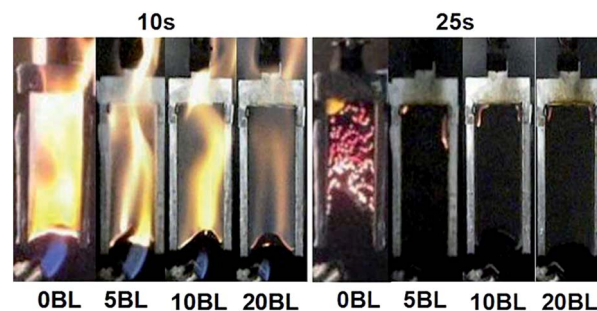


Fig. 5 Burning images of all fabrics samples respectively recorded at 10 s, and 25 s during the VFT.

Table 1 The collected data of thermal stabilities of the pure and coated fabrics were evaluated by TGA under air atmosphere

Sample	Add-on (wt%)	T_{onset} (°C)	$T_{\text{max}1}$ (°C)	$T_{\text{max}2}$ (°C)	Residue at 500 °C (wt%)	Residue at 600 °C (wt%)
Uncoated	—	337	362	447	7.4	3.0
5BL	1.7	352	371	628	9.2	5.3
10BL	2.9	359	376	620	13.6	6.5
20BL	5.9	346	357	591	20.4	9.7

Table 2 The combustion behavior data of all samples (all fabrics samples were measured three times, and the average values and standard deviations of each sample were listed)

Sample	Burning time		Afterglow		Residue	
	μ (s)	δ	μ (s)	δ	μ (wt%)	δ
Uncoated	27	0.816	18	0.816	—	—
5BL	23	1.633	0	0	3.5	0.163
10BL	23	0.816	0	0	4.5	0.082
20BL	22	0.816	0	0	5.6	0.163

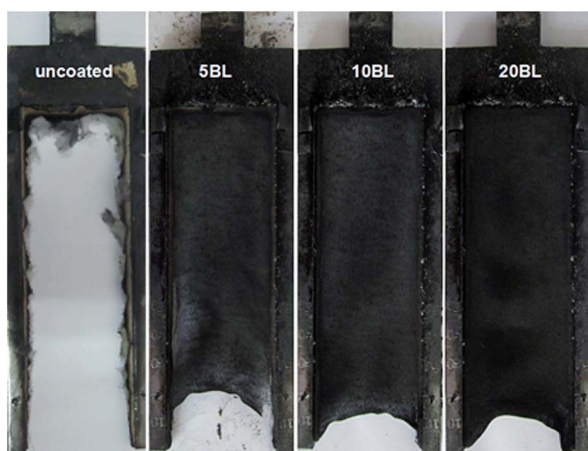


Fig. 6 Images of all fabrics samples after VFT.

retardant effect on cotton fabric and the flame retardant performance increases with the increase of bilayer number.

To investigate the flame-retardant mechanism of the assembly coating, the residue chars of the coated fabrics after VFT were observed by SEM. As shown in Fig. 7, the uncoated fabric has no residue left after VFT; however, the assembly coated fabrics still maintain the wave structure after burning. At higher magnification, it could be found that cotton fibers curl and shrink during the combustion process, especially for 5BL and 10BL coated samples. After burning, lots of CNTs networks appeared on the fibers and became more obvious with the increase of bilayer number, indicating the formation of dense physical barrier layer which could prevent cotton fabrics decomposing from fire to a certain degree. Based on our previous report,²³ it could be concluded that present PHMGP/PA-CNT coating is a mechanism combination of intumescent flame retardant and physical barrier, and owns more fire resistant performance compared to that of PHMGP/PA coating.²³ The contribution of CNTs may be attributed to two aspects: on one hand, the increase physical barrier char layer further improves and perfects the fire resistant performance of cotton fabrics. On the other hand, the improved initial thermal stability by CNTs favors the occurrence of catalytic action and forms more intumescent char, although no obvious bubbles appeared in the present assembly coating. For common intumescent flame retardant system, the forming process of carbon layer and releasing of gases are simultaneous which is

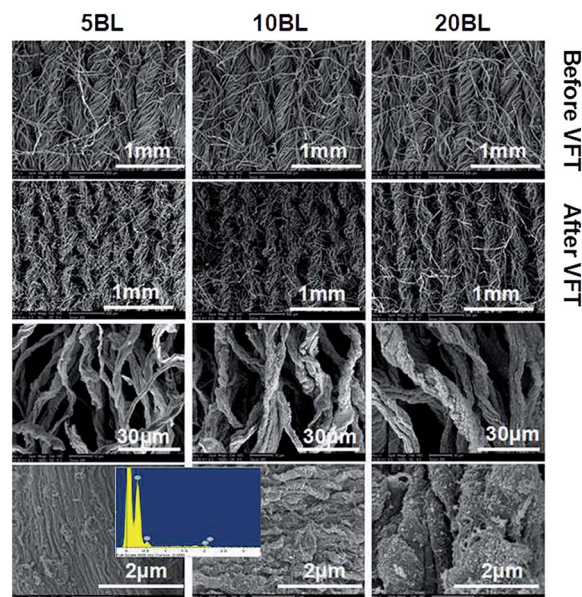


Fig. 7 SEM images of the residue char of different samples after VFT.

conductive to the forming of bubbles. In the PHMGP/PA-CNTs coating, a part of carbon layers formed by CNTs networks have been constructed on the surface of cotton fibers, and makes the disperse of gases as the gas source is more slowly in the coating layers and could form smaller inconspicuous bubbles, resulting to be difficultly observed in the SEM images. However, the detailed combustion process of PHMGP/PA-CNTs still needs to be further investigated.

FTIR is used to further analyze the residue char of different samples after burning. As shown in Fig. 8, there appear two absorption peaks around 1433 cm^{-1} and 1589 cm^{-1} corresponded to the benzene ring skeletal vibration which indicated that benzene ring was formed after burning. The absorption peaks at 806 cm^{-1} and 874 cm^{-1} are attributed to the out-of-plane vibrations of C-H which can further demonstrate the

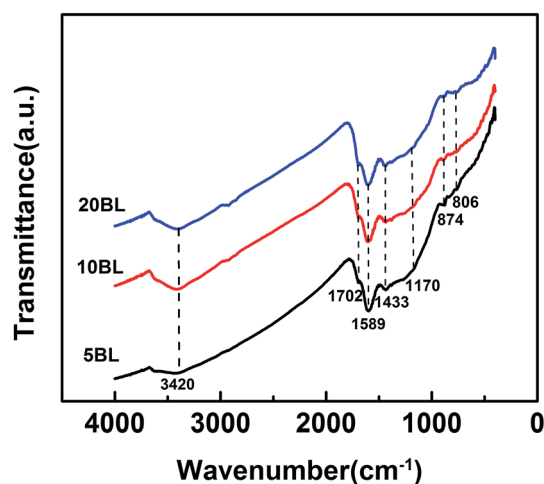


Fig. 8 FTIR spectra of the residue char of different samples after VFT.

formation of benzene ring.²³ The absorption peaks at 1170 cm^{-1} and 3420 cm^{-1} correspond to bending vibration of C–O and skeletal vibration of O–H³³ respectively which can infer a part of alcohol structure is remained. A small but clear peak appears at 1702 cm^{-1} and is attributed to C=O vibration.³⁴ Compared to the FTIR spectra before VFT, this peak becomes more obvious than that of before, and there is no peak assigned to C–O–C band in FTIR spectra after VFT but appears in FTIR before VFT. These suggest that C–O–C and C–C bands formed C=O and C=C with water deprivation respectively. The stable structures like benzene ring formed in fire, make up stable carbon layers which can protect fabric from further decomposition.

Antimicrobial properties

It is well known that a number of polymeric guanidine families have antimicrobial properties, including PHMGP.^{35–37} The antimicrobial properties of the coated fabrics were firstly evaluated by the Kirby–Bauer test,³⁸ in which *E. coli* as an important pathogenic bacterium of human was selected as the representative. As shown in Fig. 9, the coated fabric inhibits the growth of bacteria. The 5BL shows a zone of inhibition (ZOI) of 14.6 mm at the colony of 3×10^3 CFU. When the colonies are 3×10^4 and 3×10^5 , the ZOI are 13.4 and 13.3 mm, respectively. As the colony increases further to 3×10^6 , the ZOI reduces to 12.1 mm. This result shows that the ZOI gradually decreases with the increasing colony of *E. coli*. Moreover, the similar tendency can also be found in the 10 and 20BL coated fabrics (see Fig. 9).

In order to further evaluate the antimicrobial performances of the coated fabrics, the inhibited colony number was calculated by the eqn (1):

$$\text{Inhibition colony number} = (r^2 - 4^2)/R^2 \times \text{CFU} \quad (1)$$

where, r and R are the radius of the zone of inhibition and bacterial growth area, respectively, and CFU represents colony forming unit. Similarly before, the inhibited colony number increases with the colony of bacteria which were reflected in

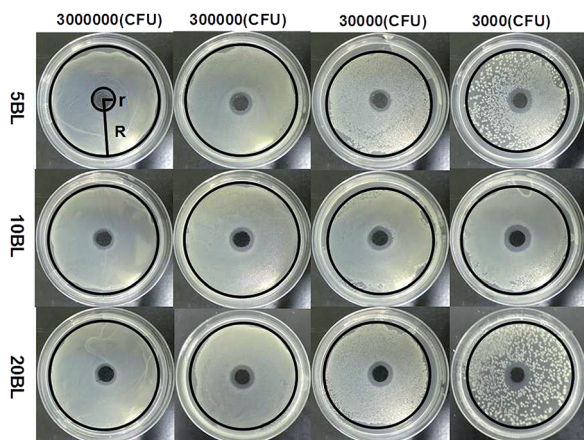


Fig. 9 The photographs of *E. coli* growth inhibition of the coating fabrics.

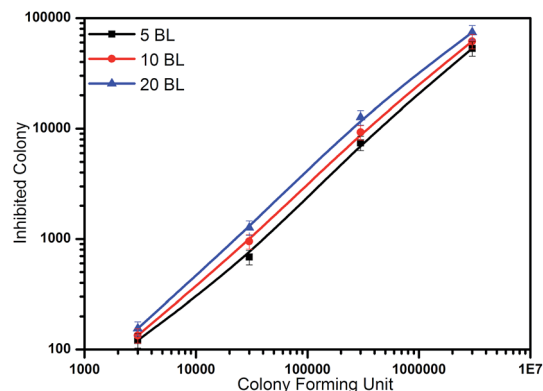


Fig. 10 The inhibited colony number of the coating fabrics as a function of the CFU of *E. coli*. Error bars reflect 15% error range.

Fig. 10. For example, the 5BL inhibits 121 colonies at the colony of 3×10^3 CFU. The inhibited colonies increase to 687 and 7337 as the colonies increase to 3×10^4 and 3×10^5 , respectively. When the colony increases further to 3×10^6 , the inhibited colonies reach up to 53 010. What's more, the 10 and 20BL show similar tendency with the growth of colony. With the colony rises to 3×10^7 , the ZOI will be approximate to the sample size, may causing large error in calculating the inhibited colony number. In view of that, the measured antimicrobial performances of the coated fabrics at the colony of 3×10^6 approaches their true antimicrobial abilities in this test method.

Fig. 11 shows the inhibited colony of three different bilayer number as a function of colony forming unit respectively. It can be seen that the 5BL inhibits the growth of 121 colonies, and the inhibited colonies are 134 for the 10BL coated fabric. As for the coated sample with 20BL, the inhibited colonies reach up to 155. It suggests that the inhibited colony increases with the growth of the bilayer number at the colony of 3×10^4 . The similar rules can also be found at other orders of magnitudes

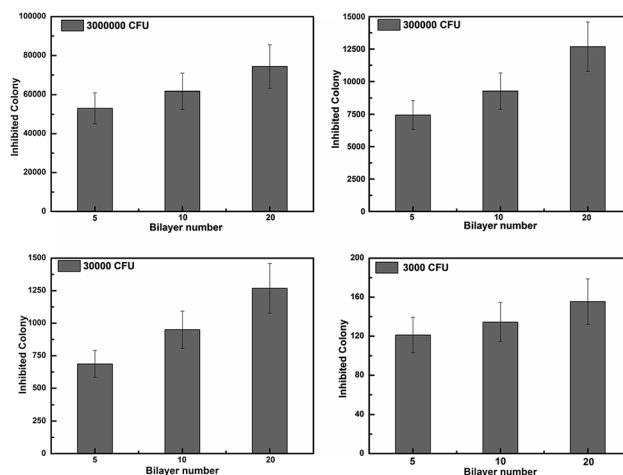


Fig. 11 The inhibited colony number of different samples for each CFU of *E. coli*. Error bars reflect 15% error range.

Table 3 The antibacterial properties of the fabric samples against *E. coli*. The error in the measured bacterial reduction is 15%

Sample	Contact time (min)	Bacterial reduction (%)
Uncoated	30	20
	60	40
5BL	30	99.67
	60	100
10BL	30	99.83
	60	100
20BL	30	99.83
	60	100

colony. All these results indicate that the antimicrobial performance of the coated fabric increases with the bilayer number. The enhanced antimicrobial property can be attributed to more PHMGP attached on the coated fabric.

In order to quantitatively assess the antimicrobial ability of PHMGP/PA-CNTs coating, a modified AATCC test method 100-2004 was adopted and the result was listed in Table 3. Bacterial reduction was calculated by the eqn (2):

$$\text{Bacterial reduction} = [(U_t - C_t)/C_t] \times 100\% \quad (2)$$

where, U_t is on behalf of the surviving bacterial colonies of uncoated fabric sample, and C_t are the surviving bacterial colonies (CFU mL⁻¹) of coated fabric samples.

It can be seen that some bacteria adsorbed on the surface of uncoated fabric died gradually with the increase of contact time. It can be explained that there is not enough nutriment to support the growth of bacteria on the surface of cotton fabric. 5BL coated fabric inhibits 99.67% *E. coli* in only 30 min contact time. With the contact time increasing to 60 min, the coated fabrics can completely inhibit *E. coli*. Furthermore, it is noted that the bacterial reduction increases slightly with the increase of BL layer number, which agrees well with the results in previous report.²³ This could be attributed that the antimicrobial action mainly occurs on the surface of coated fabrics.

Conclusions

A multifunctional coating with electrical conductivity, flame retardant and antimicrobial properties was constructed on cotton *via* LBL assembly technique. The assembly coating grows linearly in the assembly process, and the CNTs networks formed on the surface of cotton fiber endow cotton excellent electrical conductivity. Meanwhile, the assembly coating also effectively improves the thermo stability and flame retardant property of cotton. The antimicrobial assessment indicates that the assembly coating also simultaneously endows cotton antimicrobial property. This work demonstrates that LBL assembly technique is a simple and versatile method capable of endowing cotton multifunction, which can be a useful substitute to previous functional approach.

Acknowledgements

The authors are grateful to the support of National Natural Science Foundation of China (No. 51303182).

References

- 1 R. K. Iler, Multilayers of Colloidal Particles, *J. Colloid Interface Sci.*, 1966, **21**, 569–594.
- 2 Y. Lvov, G. Decher and G. Sukhorukov, Assembly of thin-films by means of successive deposition of alternate layers of DNA and poly(allylamine), *Macromolecules*, 1993, **26**, 5396–5399.
- 3 G. Decher, F. Essler, J. D. Hong, K. Lowack, J. Schmitt and Y. Lvov, New nanocomposite films for biosensors: layer-by-layer adsorbed films of polyelectrolytes, proteins or DNA, *Biosens. Bioelectron.*, 1994, **9**, 677–684.
- 4 J. Schmitt, T. Grunewald, G. Decher, P. S. Pershan, K. Kjaer and M. Losche, Internal structure of layer-by-layer adsorbed polyelectrolyte films—neutron and X-ray reflectivity study, *Macromolecules*, 1993, **26**, 7058–7063.
- 5 G. Decher, Fuzzy Nanoassemblies: Toward Layered Polymeric Multicomposites, *Science*, 1997, **277**, 1232–1237.
- 6 W. B. Stockton and M. F. Rubner, Molecular-Level Processing of Conjugated Polymers. 4. Layer-by-Layer Manipulation of Polyaniline *via* Hydrogen-Bonding Interactions, *Macromolecules*, 1997, **30**, 2717–2725.
- 7 L. Y. Wang, Z. Q. Wang, X. Zhang, J. C. Shen, L. F. Chi and H. Fuchs, A new approach for the fabrication of an alternating multilayer film of poly(4-vinylpyridine) and poly(acrylic acid) based on hydrogen bonding, *Macromol. Rapid Commun.*, 1997, **18**, 509–514.
- 8 M. Schutte, D. G. Kurth, M. R. Linford, H. Colfen and H. Mohwald, Metallo-supramolecular thin polyelectrolyte films, *Angew. Chem., Int. Ed.*, 1998, **37**, 2891–2893.
- 9 G. B. Sukhorukov, E. Donath, H. Lichtenfeld, E. Knippel, M. Knippel, A. Budde and H. Mohwald, Layer-by-layer self assembly of polyelectrolytes on colloidal particles, *Colloids Surf., A*, 1998, **137**, 253–266.
- 10 R. A. Caruso, A. Susa and F. Caruso, Multilayered Titania, Silica, and Laponite Nanoparticle Coatings on Polystyrene Colloidal Templates and Resulting Inorganic Hollow Spheres, *Chem. Mater.*, 2001, **13**, 400–409.
- 11 W. H. Jiang, G. J. Wang, Y. N. He, Y. L. An, X. G. Wang, Y. L. Song and L. Jiang, Properties of photo-responsive superhydrophobic azobenzene multilayers fabricated by electrostatic self-assembly, *Chem. J. Chin. Univ.*, 2005, **26**, 1360–1362.
- 12 Y. C. Li, S. Mannen, A. B. Morgan, S. C. Chang, Y. H. Yang, B. Condon and J. C. Grunlan, Intumescent All-Polymer Multilayer Nanocoating Capable of Extinguishing Flame on Fabric, *Adv. Mater.*, 2011, **23**, 3926–3931.
- 13 L. Galina, K. Christopher, A. A. Cain and J. C. Grunlan, Clay-Chitosan Nanobrick Walls: Completely Renewable Gas Barrier and Flame-Retardant Nanocoatings, *ACS Appl. Mater. Interfaces*, 2012, **4**, 1643–1649.

- 14 F. Carosio, A. D. Blasio, J. Alongi and G. Malucelli, Green DNA-based flame retardant coatings assembled through layer by layer, *Polymer*, 2013, **54**, 5148–5153.
- 15 H. B. Chena, Y. Z. Wang, M. S. Soto and D. A. Schiraldi, Low flammability, foam-like materials based on ammonium alginate and sodium montmorillonite clay, *Polymer*, 2012, **53**, 5825–5831.
- 16 S. T. Dubas, P. Kumlangduksana and P. Potiyaraj, Layer-by-layer deposition of antimicrobial silver nanoparticles on textile fibers, *Colloids Surf., A*, 2006, **289**, 105–109.
- 17 S. C. Chang, R. P. Slopek, B. Condon and J. C. Grunlan, Surface Coating for Flame-Retardant Behavior of Cotton Fabric Using a Continuous Layer-by-layer Process, *Ind. Eng. Chem. Res.*, 2014, **53**, 3805–3812.
- 18 S. S. Ugur, M. Sariisik and A. H. Aktas, Nano-Al₂O₃ multilayer film deposition on cotton fabrics by layer-by-layer deposition method, *Mater. Res. Bull.*, 2011, **46**, 1202–1206.
- 19 Q. Wang and P. J. Hauser, Developing a novel UV protection process for cotton based on layer-by-layer self-assembly, *Carbohydr. Polym.*, 2010, **81**, 491–496.
- 20 L. Chen, L. Bromberg, J. A. Lee, H. Zhang, H. S. Gibson, P. Gibson, J. Walker, P. T. Hammond, T. A. Hatton and G. C. Rutledge, Multifunctional Electrospun Fabrics via Layer-by-Layer Electrostatic Assembly for Chemical and Biological Protection, *Chem. Mater.*, 2010, **22**, 1429–1436.
- 21 A. J. Mateos, A. A. Cain and J. C. Grunlan, Large-Scale Continuous Immersion System for Layer-by-Layer Deposition of Flame Retardant and Conductive Nanocoatings on Fabric, *Ind. Eng. Chem. Res.*, 2014, **53**, 6409–6416.
- 22 F. Fang, D. Z. Xiao, X. Zhang, Y. D. Meng, C. Cheng, C. Bao, X. Ding, H. Cao and X. Y. Tian, Construction of intumescent flame retardant and antimicrobial coating on cotton fabric via layer-by-layer assembly technology, *Surf. Coat. Technol.*, 2015, **276**, 726–734.
- 23 F. Fang, X. X. Chen, X. Zhang, C. Cheng, D. Z. Xiao, Y. D. Meng, X. Ding, H. Zhang and X. Y. Tian, Environmentally friendly assembly multilayer coating for flameretardant and antimicrobial cotton fabric, *Prog. Org. Coat.*, 2016, **90**, 258–266.
- 24 T. Kashiwagi, E. Grulke, J. Hilding, K. Groth, R. Harris, K. Butler, J. Shields, S. Kharchenko and J. Douglas, Thermal and flammability properties of polypropylene/carbon nanotube nanocomposites, *Polymer*, 2004, **45**, 4227–4239.
- 25 P. Podsiadlo, B. S. Shim, W. Chen, C. Doty, C. L. Xu and N. A. Kotov, Smart Electronic Yarns and Wearable Fabrics for Human Biomonitoring made by Carbon Nanotube Coating with Polyelectrolytes, *Nano Lett.*, 2008, **8**, 4151–4157.
- 26 Y. Liu, P. Liang, H. Y. Zhang and D. S. Guo, Cation-controlled aqueous dispersions of alginate-acid-wrapped multi-walled carbon nanotubes, *Small*, 2006, **2**, 874–878.
- 27 C. D. Zhang, L. M. Price and W. H. Daly, Synthesis and Characterization of a Trifunctional Aminoamide Cellulose Derivative, *Biomacromolecules*, 2006, **7**, 139–145.
- 28 C. Chung, M. Lee and E. K. Choe, Characterization of cotton fabric scouring by FT-IR ATR spectroscopy, *Carbohydr. Polym.*, 2004, **58**, 417–420.
- 29 Y. M. Zhang, J. M. Jiang and Y. M. Chen, Synthesis and antimicrobial activity of polymeric guanidine and biguanidine salts, *Polymer*, 1999, **40**, 6189–6198.
- 30 M. Ionita, M. A. Pandele and H. Iovu, Sodium alginate/graphene oxide composite films with enhanced thermal and mechanical properties, *Carbohydr. Polym.*, 2013, **94**, 339–344.
- 31 A. B. Rossa, C. Halla, K. Anastasakisa, A. Westwoodb, J. M. Jonesa and R. J. Crewc, Influence of cation on the pyrolysis and oxidation of alginates, *J. Anal. Appl. Pyrolysis*, 2011, **91**, 344–351.
- 32 K. Chrissafis, Detail kinetic analysis of the thermal decomposition of PLA with oxidized multi-walled carbon nanotubes, *Thermochim. Acta*, 2010, **511**, 163–167.
- 33 Y. H. Li, F. Q. Liu, B. Xia, Q. J. Du, P. Zhang, D. C. Wang, Z. H. Wang and Y. Z. Xia, Removal of copper from aqueous solution by carbon nanotube/calcium alginate composites, *J. Hazard. Mater.*, 2010, **177**, 876–880.
- 34 F. Carosio, A. D. Blasio, J. Alongi and G. Malucelli, Green DNA-based flame retardant coatings assembled through layer by layer, *Polymer*, 2013, **54**, 5148–5153.
- 35 P. Broxton, P. M. Woodcock and P. Gilbert, A study of the antibacterial activity of some polyhexamethylene biguanides towards *Escherichia coli* ATCC 8739, *J. Appl. Bacteriol.*, 1983, **54**, 345–353.
- 36 P. Broxton, P. M. Woodcock and P. Gilbert, Binding of some polyhexamethylene biguanides to the cell envelope of *Escherichia coli* ATCC 8739, *Microbios*, 1984, **41**, 15–22.
- 37 P. Gilbert, P. J. Collier and M. R. W. Brown, Influence of Growth Rate on Susceptibility to Antimicrobial Agents: Biofilms, Cell Cycle, Dormancy, and Stringent Response, *Antimicrob. Agents Chemother.*, 1990, **34**, 1865–1868.
- 38 D. Lee, R. E. Cohen and M. F. Rubner, Antibacterial properties of Ag nanoparticle loaded multilayers and formation of magnetically directed antibacterial microparticles, *Langmuir*, 2005, **21**, 9651–9659.